Experimental study of beam to concrete-filled elliptical steel tubular column connections

J. Yang, T. Sheehan*, X.H. Dai & D. Lam

School of Engineering, University of Bradford, Richmond Road, Bradford BD7 1DP, United Kingdom

Abstract: This paper investigated the rotation behaviour of simply bolted I-beam to concrete-filled elliptical steel tubular (CFEST) column connections experimentally. Ten different joint assemblies were tested to failure, with a constant axial compressive load applied to the column and upwards concentrated loads at the beam ends. All of the steel tubes were hot-finished and had a cross-sectional aspect ratio of 2. The orientation of the column and the arrangement of the stiffening plates were taken into consideration. Moment versus rotation relationships and failure modes were compared for each joint, highlighting the benefits of using core concrete and stiffeners in these connections.

Keywords: Concrete-filled columns; Elliptical hollow section; Beam to column connections; Rotation behaviour; Experimental study.

1. Introduction

Concrete-filled steel tubular columns (CFST) are widely used in frame structures owing to their superior structural performance. The CFST column is an optimum combination of different materials, steel and concrete. With the confinement effect provided by the steel tube, the core concrete will obtain higher strength, while in turn, the concrete may eliminate or delay the commencement of local buckling in the steel tube. Additionally, the outer steel tube could be the formwork when casting concrete, which is more economic compared with

*Corresponding author, Phone: +44(0)1274235779; Email: t.sheehan@bradford.ac.uk

reinforced concrete and enables rapid construction.

The most common cross-sectional shapes of CFST columns until now have been circular, square and rectangular. Only recently did a new range of elliptical hollow sections (EHSs) become available in the manufacturing industry and subsequently be introduced into building structures. The sectional sizes of EHSs range from 120×60×3.2 mm up to 500×250×16 mm in Grade S355J2H and the minimum yield strength is 355 MPa [1]. The EHS not only has a varied and interesting appearance which fulfils the aesthetic purpose in design, but also provides potential structural efficiency. With two different principal axes, it has better bending capacity compared with a circular hollow section (CHS) of the same area or weight [2]; its closed shape offers high torsional stiffness [3] and high resistance to lateral torsional buckling [4].

With the merits mentioned above, EHS has been applied in several cases, e.g. Heathrow Airport in London and Society Bridge in Scotland. However, there is a lack of appropriate design rules to ensure the safety and economy of utilizing EHS in construction, which hinders its widespread application. Currently, existing research has focused on the behaviour of hollow EHSs [5, 6] and concrete-filled EHSs [7-10]. However, these investigations did not involve the interaction between members in a connection.

The first experiment on welded EHS tubular joints dates back to 2003; Bortolotti et al [11] and Pietrapertosa and Jaspart [12] tested the brace-to-chord N- and X-joints where the brace was welded on the wide side of the EHS chord. Choo et al. [13] then furthered the study based on experimental results of welded EHS X-connections covering a wider range of variables through numerical analysis. It is concluded that with appropriate EHS orientation,

axially loaded EHS connections can achieve higher capacities than equivalent CHS connections with the same brace and chord sectional areas. Willibald et al [14] investigated the behaviour of gusset-plate connections to EHSs where the branch/through plate was arranged in either the longitudinal or transverse direction of the EHS steel tube; and was connected on the wide/narrow side of the EHS. It is found that the yield strength of the through plate connection is approximately twice that of the branch plate connection or more. Connections with composite tubular columns have also been studied based on varied connection types and loading conditions. Elremaily and Azizinamimi [15] conducted laboratory tests on through beam connections under monotonic loading with the beam web attached to the web cleat plate through both fabrication bolts and fillet welds. Wang et al. [16, 17] investigated the static and hysteretic behaviour of flush end plate joints to CFST columns using high strength blind bolts. Cheng et al. [18] reported static behaviour of CFST connections with square columns stiffened with internal diaphragms. Han and Li [19] tested connections with a reinforced concrete (RC) slab reinforced by an external ring, under seismic loading; Song and Han [20] provided a numerical investigation on the post-fire behaviour of such CFST connections. However, the fabrication of these connection types is always complicated and time-consuming. And it is even more difficult to repeat the investigations for connections with EHSs due to the complexity of geometry. Lam and Dai [21] conducted a numerical study using an ABAQUS solver on four types of easy-to-construct beam to elliptical column connections. The effect of some important parameters on the structural behaviour of the connections was observed.

This paper follows on from the above numerical study and starts to explore the behaviour of

simply bolted I-beam to concrete-filled elliptical column connections experimentally, employing either fin plates or a through plate. The aim is to eventually find out solutions to these kinds of connections for design. Several joint configurations, with or without concrete core/stiffening plates in the columns, were taken into consideration. A total of ten specimens were tested to failure with the columns bending in the major or minor axis direction. The moment versus rotation relationships and failure modes of ten specimens were addressed and analysed; the effect of core concrete and stiffening plates on bending behaviour of simply bolted beam to elliptical column connections was highlighted.

2. Experimental study

2.1 Specimen types and details

Of all the specimens, five different joint assemblies (named after Type-A, B, C, D, and Type-E) have been considered, as illustrated in Fig. 1. Each type of assembly comprised one specimen with a hollow EHS column and another specimen with an EHS column filled with concrete, to explore the enhancement of concrete infill on the structural behaviour of these joints. All EHS columns were manufactured from Grade S355 steel with a minimum yield strength of 355 MPa. Due to the different axes of the EHS tube, two configurations of joint can be obtained as shown by Type-B and Type-D joints. As it is difficult to arrange stiffeners in both major and minor axis directions, only one stiffener plate is adopted for each joint, as seen in Type-A and Type-E connections. For minor axis connection Type-C, a through plate, functioning as both fin plate and stiffener, is adopted to ensure the continuous stiffness of the joint. The five joint assemblies are described as follows:

Type-A: Major axis connection with stiffener

Two fin plates (220×110×10 mm) in the major axis direction and a stiffener plate (220×140×10 mm) in the minor axis direction;

Type-B: Major axis connection without stiffener

Two fin plates (220×110×10 mm) in the major axis direction and no stiffener plate;

Type-C: Minor axis through plate connection

A whole plate (220×320×10 mm) through the column function as both fin plate and stiffener plate in the minor axis direction;

Type-D: Minor axis connection without stiffener

Two fin plates (220×110×10 mm) in the minor axis direction and no stiffener plate;

Type-E: Minor axis connection with stiffener

Two fin plates (220×110×10 mm) in the minor axis direction and a stiffener plate (220×140×10 mm) in the major axis direction.

Fig. 1. Joint assemblies (Cross-sectional view)

For a typical connection, two beams were connected with the column using fin plates with three M20 Gr. 8.8 or Gr. 10.9 bolts on each side; the fin plate is welded by using fillet weld (weld size is 6 mm) at the mid-height of the elliptical column. For Type-C connection, the through plate was run through the pre-slotted EHS column and was then welded to external face of column (6mm fillet welds). Prior to conducting the experiments, the actual dimensions of EHS columns were measured. Mean values are listed in Table 1, where 2a, 2b, t and L mean the shorter diameter, longer diameter, thickness and length of the EHS column, respectively; hollow joints named by Joint-A, Joint-B, etc., while the concrete-filled

counterparts were Joint-AC, Joint-BC, etc. All beams adopted in the specimens are 900 mm long, with beam sections of 305×127×48 UB.

Table 1 Mean measured values of EHS column dimensions (mm)

Two batches of concrete were made with the same mix design given in Table 2, to cast all of the specimens. The concrete cube tests were conducted and an average of 28-day strength of 37 MPa and test-date strength of 42 MPa were obtained.

Table 2 Concrete mix specification design and compressive strength

2.2 Testing procedure

The typical test setup can be seen in Fig. 2. All tests were carried out in the heavy structures lab of the School of Engineering, University of Bradford. A compressive load which was approximately equals to 40% of the column resistance was firstly applied at the top column end using a 2500 kN actuator (Jack-3) as shown in Fig. 2. Two 1000 kN hydraulic actuators (Jack-1 and Jack-2) were then employed to exert an upwards concentrated force at each beam end, replacing the distributed load that would occur from a concrete floor slab in a real frame structure. Specially designed roller bearings (see Fig. 3) were employed, connected to the tops of Jacks 1 and 2. The curved rollers allowed the beams to rotate in the plane of the test-rig and plates were welded to the sides of the rollers to constrain out-plane freedoms of the bottom flanges to some extent. The initial distance from the edge of the beam flange to the loading point was 50 mm. A slotted and reusable steel cap was adopted at the top end of the column. On the top of this special cap, as depicted in Fig. 4(a), a circular groove slightly bigger than

the load cell was carved to slot the loading cell into while an elliptical slot (see Fig. 4(b)) was made on the opposite side to cover the top of the EHS column to constrain sliding parallel to the orientation of the I-beams and out-of-plane movement of the specimen. For the bottom end of the EHS column, two clamps were employed as shown in Fig. 4(c), providing a semi-rigid boundary condition for the connections. It is worth mentioning that for the concrete-filled columns, plaster was used to fill the gap caused by shrinkage of the concrete after casting and to make sure that the compressive load was applied evenly to both steel tube and concrete.

Fig. 2. Typical test setup

Fig. 3. Roller bearing

Fig. 4. Boundary conditions: (a) Top end: connecting actuator; (b) Top end: connecting EHS column; (c) Bottom end (using clamps).

2.3 Instrumentation

Several linear variable displacement transducers (LVDTs) and strain gauges were used to measure displacements and strains of selected locations, separately, as illustrated in Fig. 5. LVDTs named from *L*-1 to *L*-4 were arranged to measure the rotation of the beams. *L*5-*L*8 were placed at the bottom flanges of the beams to check whether or not beam bending occurred and also to provide an alternative method to derive the rotations of the joints. *L*9 and *L*10, employed to measure the shortening of the elliptical columns, were placed directly

underneath the top steel cap. *L*11-*L*14 were used to capture the concave or convex deformations on the sides of the EHS column tubes directly above and below the connections. Rotations of the I-beam to column connections can be calculated using the displacements measured by *L*1-*L*8 and the equation is listed as follows:

$$\theta = \frac{1}{2}\left(\theta_{1-4} + \theta_{5-8}\right) = \frac{1}{2}\left[Arc\tan\left(\frac{D^{+}}{2s}\right) + Arc\tan\left(\frac{D^{-}}{I/3}\right)\right]$$

Where θ denotes the rotation of the elliptical column to beam connection; $\theta_{1\text{-}4}$ and $\theta_{5\text{-}8}$ refer to the rotations calculated by the displacements from *L*1-*L*4 and *L*5-*L*8, respectively; D^{+} is the sum of the displacements obtained from *L*1 and *L*3 (left side, Jack-1) or *L*2 and *L*4 (right side, Jack-2); D^{-} is the difference between the displacements measured by *L*5 and *L*6 (left side, Jack-1) or *L*7 and *L*8 (right side, Jack-2); *s* is the central spacing of the bolts with a value of 60 mm, *I* equals to 800 mm, which is the horizontal distance between the beam load centre to the joint (bolt) centre.

Gauges named from *C*1 to *C*9 were used to measure either longitudinal or circumferential strains on the column, while gauges named from "10" to "16" were those located on fin plates, either near fillet welds connecting the fin plates to the column or adjacent to bolt holes to monitor the critical strain. Similar arrangements were adopted for the other nine specimens.

Fig. 5. Positions of Strain Gauges & LVDTs (Type-A; mm)

3. Experimental results and comparisons

3.1 Moment versus rotation curves

Fig. 6 shows the comparisons between moment versus rotation relationships for each joint, where the moments are equal to 0.8 meters (distance between beam end loading centre and

beam-column connection centre) × the concentrated load at the beam end and the rotation is calculated using the above mentioned equation. The lines with hollow square or circle data points represent results of unfilled connections while those with filled points refer to the results from concrete-filled connections; black curves denote results from the left hand actuator Jack-1 and red curves denote results from the right hand actuator Jack-2. The initial gap from the beam end to the column surface for all of the specimens was designed to be 10 mm, but differences in the gap size were observed between the left hand side and right hand side in each connection and between different specimens. This imperfection led to the non-synchronous moment-rotation response of the two sides although the two beams were compressed under same loading scheme. In Fig. 6 (e), another set of data, represented by filled triangle data points, was given because a repeat test of Joint-EC was conducted using a higher grade of bolt.

As can be seen from Fig. 6, friction, which existed between the fin plates, beams and bolts, was in control in the initial stage of the test. The rotation of the connection was quite low and the slope was nearly constant, with the column, beam and bolts working well together. Then, the moment climbed slowly with increasing rotation showing that slip occurred after the applied load exceeded the friction. After that, the curves progressed to the next phase where the slope increased, the bolts and holes compressed each other until the failure of the connections. But different curve slopes were observed for concrete-filled and hollow columns after the beam end touched the column surface; the curve slopes of filled connections were steeper due to the enhancement provided by the concrete core to the rotation capacity. The sudden drops seen in the curves were caused by the shear failure of one or more bolts in the

final stage of the experiments.

Fig. 6. Moment versus rotation relationships

The lower moment between the two sides of joint is adopted to be the ultimate bending moment for safety concerns. The ultimate moments M_u, corresponding to rotations θ_u and the ratio of the ultimate moment between hollow and concrete-filled specimens, $M_{u\text{-hollow}}/M_{u\text{-filled}}$ for all of the specimens are given in Table 3. The enhancement of the ultimate moment ranged from 1.91 to 5.19, and the corresponding rotations of the hollow connections were normally bigger than their concrete-filled counterparts. Therefore, it can be concluded that core concrete in the column can improve the moment behaviour of elliptical column to I-beam connections considerably and the most notable cases were those without stiffening plates (Joint-BC and Joint-DC).

As expected, the moment capacity of Joint-A is significantly higher than that of Joint-B owing to the enhancement of the stiffener plate in the minor axis direction of the EHS tube. However, the ultimate moment of Joint-AC was slightly lower than that of the unstiffened counterpart Joint-BC. The reason may be that the failure of the connection with core concrete was governed by bolt failure. Additionally, the benefit of using concrete in the column was more notable in the unstiffened Type-B connections than Type-A connections, due to the contribution of stiffeners to the minor axes of EHS columns.

Among all of the specimens, through plate Type-C connections exhibited the highest capacity in both hollow connections and the concrete-filled group, although they failed at a lower joint rotation. The explanation is that the through plate endured significantly more load transferred

from the beam ends. By comparing the results of Joint-D and Joint-E, it can be concluded that although in an EHS tube, the stiffness in the major axis direction is higher than that in the minor axis direction, moment capacity of the minor axis connection can still be enhanced by welding a stiffener plate in the major axis direction. But this conclusion did not apply to the equivalent concrete-filled connections. Similarly to major axis connections, the capacity of Joint-DC without stiffeners was slightly higher than the stiffened counterpart Joint-EC.

Table 3 Ultimate moments, rotations and failure modes

3.2 Failure modes

The failures of all the specimens are illustrated in Fig. 7-11. After the tests, a portion of the steel tube was removed from the concrete-filled columns, in order to inspect the condition of the concrete core (Fig. 7(e), Fig. 8(c), Fig. 9(c), Fig. 11(e)). For hollow specimens, it was found that local buckling failure (see Fig. 7(c)) occurred on the column surface near the joint portion with perpendicular compression for connections without concrete. Although Joints-A, C, and E had stiffeners in either the minor or major axis direction, inwards local buckling still occurred near the top section of the connection owing to the direct compression from the top flange of the beam (see Fig. 7(a), Fig. 9(a) and Fig. 11(a)). This phenomenon disappeared in the corresponding concrete-filled connections. The core concrete mitigated the severe deformations that occurred in the hollow columns (Fig. 7(b)), while instead, one or more bolts failed in the final stage of the experiments for connections with concrete infill. Shear failure of one bolt is shown in Fig. 7(d).

An approximately square cross-sectional shape was obtained eventually in the Joint-A column, caused by compressive load transferred from the beam, as depicted in Fig. 7(c). Tearing

failure on the tube wall near the left fin plate was found in the later stage of the test for Joint-A. In contrast, there was no obvious local failure and no cracks in the core concrete (see Fig. 7(e)) which means that the stiffener, core concrete and steel tube worked really well in this case.

Similar deformation was observed at the upper portion of the Joint-B column, but an elliptical cross-sectional shape with a higher aspect ratio was obtained near the bottom of the connection owing to the direct tension force and the absence of a stiffening plate. In contrast to Joint-AC, cracks occurred on the core concrete of Joint-BC around the upper worst section initiating at the right hand side of the ellipse, as shown in Fig. 8(c). Both of the bottom bolts of Joint-BC failed in shear.

Inward local failure of Joint-C and the most severely deformed section are shown in Fig. 9(a) and (b), respectively. With the exception of these locations, there is no obvious deformation in the Joint-C column and no cracks in the core concrete of Joint-CC (Fig. 9(c)). The reason is that together with the bolts, the through plate in the minor axis direction, which combined the stiffener and fin plates, endured almost the whole shear force and moment transferred from the beam before beam end touched the column face. The load was transferred from the beam to the bolts and then to the through plate. Owing to the external fillet welds between the “fin plate” and the column face, the EHS tube wall was subjected to compressive force near the upper section and tensile force near the bottom part. However, the “stiffener plate” helped to endure most of the compressive or tensile load, thus large concave or convex deformations occurred in the EHS column around the connection and cracks in core concrete were prevented. Shear force increased with the increasing of joint rotation, and thus leaded to

failure of bolts. In particular, two bottom bolts of Joint-C failed while those in Joint-A and –B did not, which verified the above explanation.

Comparison of failure modes of Type-D connections can be seen in Fig. 10. Inward local buckling was observed in the Joint-D column, in contrast, no deformation occurred in the steel tube but cracking occurred throughout the core concrete at the same position. The concrete failure of Joint-DC was more severe than that of Joint-BC because it was subjected to bending in the weaker axis direction. Moreover, for Joint-DC, the bottom and middle bolts at the left side failed in sequence eventually, along with the tear failure of the column wall on the right side.

Failures of Type-E connections are illustrated in Fig. 11. Gr. 8.8 bolts were used firstly in this joint assembly. For the unfilled connection Joint-E, inward local buckling occurred on the elliptical column tube (see Fig. 11(a)-(b)), while the bottom bolts at both sides of Joint-EC failed and small cracks initiated in the column surface near the bottom of the fin plates. Expecting better bending capacity, Gr. 10.9 bolts were then adopted to repeat the experiment of Joint-EC. However, the bottom and middle bolts at the left side failed in sequence eventually, accompanied with extension of the cracks on the right hand side (see Fig. 11(d)). Similar to Joint-AC and Joint-CC with stiffeners in the columns, no severe cracks were observed in the core concrete of Joint-EC as shown in Fig. 11(e).

Fig. 7. Failure of Type-A connections: (a) Joint-A; (b) Joint-AC; (c) Worst section of Joint-A; (d) Bolt failure of Joint-AC; (e) Core concrete of Joint-AC

Fig. 8. Failure of Type-B connections: (a) Joint-B; (b) Bottom cross-section of Joint-B column; (c) Core concrete of Joint-BC

Fig. 9. Failure of Type-C connections: (a) Joint-C; (b) Top cross-section of Joint-C column; (c) Core concrete of Joint-CC

Fig. 10. Failure of Type-D connections

Fig. 11. Failure of Type-E connections: (a) Joint-E; (b) Top section of Joint-E column; (c) Initial cracks of Joint-EC; (d) Fracture failure of Joint-EC; (e) Core concrete of Joint-EC

4. Conclusions

A number of experiments were conducted to investigate the rotation behaviour of simple bolted beam to elliptical column connections. Based on the experimental results, the typical failure mode of the connections with hollow columns was found to be inward local buckling of the column surface near the upper portion of the joints, though stiffeners were arranged in either the major or minor axis direction in some cases. However, the inward deformation was eliminated by the core concrete. Instead, shear failure of the bolts governed the ultimate rotation capacity of the joints with concrete infill.

According to the moment versus rotation responses of beam to elliptical column connections, friction was in control in the initial stage with the friction force existing between fin plates, beams and bolts. In this section, the rotation of the connection was quite low but the slope of the moment-rotation curves was nearly constant, with the column, beam and bolts working well together. Then, slippage occurred when the load applied was bigger than the friction force, and the moment climbed slowly with the increase of rotation. Afterwards, the bolts, the bolt holes in the fin plates and the beam webs acted together in resisting the load until the joints failed in one of the modes described previously.

For all of the joint assemblies, connections with concrete-filled columns had much higher moment capacity than their unfilled counterparts. The enhancement in moment ranged from 1.91 to 5.19. Additionally, a minor axis through plate connection was found to have higher stiffness and better moment capacity, hence this joint type was recommended for minor axis beam to elliptical column connections.

References

1. CEN, *Hot finished structural hollow sections of non-alloy and fine grain steels-Part 2: Tolerances, dimensions and sectional properties.* EN 10210-2:2006(E), European Committee for Standardization, Brussels, Belgium, 2006.
2. Packer, J.A., *Going elliptical.* Modern Steel Construction, American Institute of Steel Construction, 2008. March.
3. Chan, T.M. and Gardner, L., *Bending strength of hot-rolled elliptical hollow sections.* Journal of Constructional Steel Research, 2008. 64(9): p. 971-986.
4. Nowzartash, F. and Mohareb, M., *Plastic interaction relations for elliptical hollow sections.* Thin-Walled Structures, 2009. 47(6-7): p. 681-691.
5. Ruiz-Teran, A.M. and Gardner, L., *Elastic buckling of elliptical tubes.* Thin-Walled Structures, 2008. 46(11): p. 1304-1318.
6. Chan, T.M. and Gardner, L., *Compressive resistance of hot-rolled elliptical hollow sections.* Engineering Structures, 2008a. 30(2): p. 522-532.
7. Yang, H., Lam, D. and Gardner, L., *Testing and analysis of concrete-filled elliptical hollow sections.* Engineering Structures, 2008. 30(12): p. 3771-3781.
8. Sheehan, T., Dai, X.H., Chan, T.M. and Lam, D., *Structural response of concrete-filled elliptical steel hollow sections under eccentric compression.* Engineering Structures, 2012. 45: p. 314-323.
9. Dai, X. and Lam, D., *Numerical modelling of the axial compressive behaviour of short concrete-filled elliptical steel columns.* Journal of Constructional Steel Research, 2010. 66(7): p. 931-942.
10. Jamaluddin, N., Lam, D., Dai, X.H. and Ye, J., *An experimental study on elliptical concrete filled columns under axial compression.* Journal of Constructional Steel Research, 2013. 87: p. 6-16.
11. Bortolotti, E., Jaspart, J.-P., Pietrapertosa, C., Nicaud, G., Petitjean, P.D. and Grimault, J.P., *Testing and modelling of welded joints between elliptical hollow sections.* Proceedings of the 10th International Symposium on Tubular Structures, Madrid. Taylor & Francis, London, 2003: p. 259–266.
12. Pietrapertosa, C. and Jaspart, J.P., *Study of the behaviour of welded joints composed of elliptical hollow sections.* Proceedings of the 10th International Symposium on Tubular Structures, Madrid. Taylor & Francis, London, 2003: p. 601–608.
13. Choo, Y.S., Liang, J.X. and Lim, L.V., *Static strength of elliptical hollow section*

X-joint under brace compression. Proceedings of the 10th International Symposium on Tubular Structures, Madrid. , 2003: p. 253–258.

14. Willibald, S., Packer, J.A., Voth, A.P. and Zhao, X., *Through-plate joints to elliptical and circular hollow sections.* Tubular Structures (conference), 2006.
15. Elremaily, A. and Azizinamini, A., *Experimental behavior of steel beam to CFT column connections.* Journal of Constructional Steel Research, 2001. 57: p. 1099-1119.
16. Wang, J.-F., Han, L.-H. and Uy, B., *Behaviour of flush end plate joints to concrete-filled steel tubular columns.* Journal of Constructional Steel Research, 2009a. 65(4): p. 925-939.
17. Wang, J.-F., Han, L.-H. and Uy, B., *Hysteretic behaviour of flush end plate joints to concrete-filled steel tubular columns.* Journal of Constructional Steel Research, 2009b. 65(8-9): p. 1644-1663.
18. Cheng, C.-T., Chan, C.-F. and Chung, L.-L., *Seismic behavior of steel beams and CFT column moment-resisting connections with floor slabs.* Journal of Constructional Steel Research, 2007. 63(11): p. 1479-1493.
19. Han, L.-H. and Li, W., *Seismic performance of CFST column to steel beam joint with RC slab: Experiments.* Journal of Constructional Steel Research, 2010. 66(11): p. 1374-1386.
20. Song, T.-Y. and Han, L.-H., *Post-fire behaviour of concrete-filled steel tubular column to axially and rotationally restrained steel beam joint.* Fire Safety Journal, 2014. 69: p. 147-163.
21. Lam, D. and Dai, X., *Finite Element modelling of beam to concrete filled elliptical steel column connections.* Tubular Structures XIV. Gardner (Ed.), 2012. Taylor and Francis Group, London, ISBN 978-0-415-62137-3: p. 289-296.

Table 1 Mean measured values of EHS column dimensions (mm)

Specimen ID	2*a*	2*b*	*L*	*t*	Specimen ID	2*a*	2*b*	*L*	*t*
Joint-A	198.43	99.52	1500	5.05	Joint-AC	198.60	101.89	1499	4.97
Joint-B	200.01	101.51	1487	4.92	Joint-BC	198.47	101.57	1498	5.01
Joint-C	198.50	100.50	1498	4.88	Joint-CC	198.21	101.42	1498	5.02
Joint-D	197.78	102.03	1497	4.54	Joint-DC	198.50	101.62	1500	5.05
Joint-E	197.82	102.10	1495	4.75	Joint-EC	198.11	101.58	1495	5.17

Table 2 Concrete mix specification design and compressive strength

Water (kg/m^3)	Cement (kg/m^3)	Coarse aggregate (kg/m^3)	Fine aggregate (kg/m^3)	Compressive strength at 28 days (MPa)	Compressive strength on testing day (MPa)
225	402	1027	715	37	42

Table 3 Ultimate moments, rotations and failure modes

Specimen ID	M_u (kN·m)	θ_u (rad)	$M_{u,filled}/M_{u,hollow}$	Failure mode description
Joint-A	22.3	0.200	-	Local buckling
Joint-AC	43.8	0.110	1.96	Bolt shear failure
Joint-B	16.0	0.100	-	Local buckling
Joint-BC	49.6	0.120	3.10	Bolt shear failure
Joint-C	30.0	0.110	-	Local buckling
Joint-CC	57.2	0.110	1.91	Bolt shear failure
Joint-D	8.4	0.120	-	Local buckling
Joint-DC	43.6	0.110	5.19	Bolt shear failure
Joint-E	13.3	0.180	-	Local buckling
Joint-EC	33.8	0.130	2.55	Bolt shear failure
Joint-EC (repeat)	41.4	0.130	3.11	Bolt shear failure

Note: Local buckling occurred in EHS column surface near the upper portion of the joints.

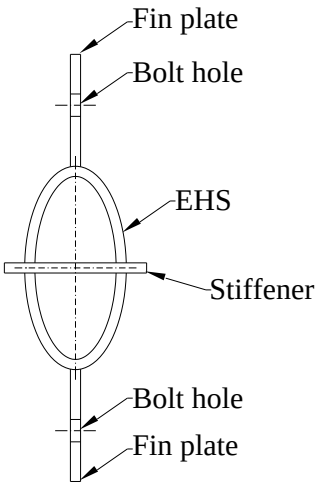

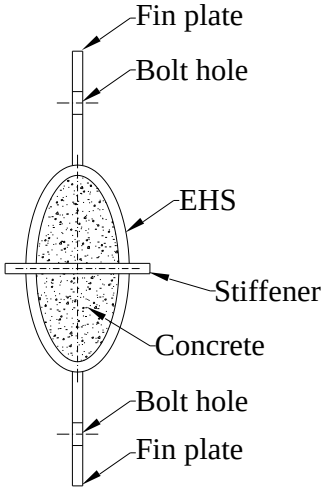

(a) Type-A: Major axis connection with stiffener

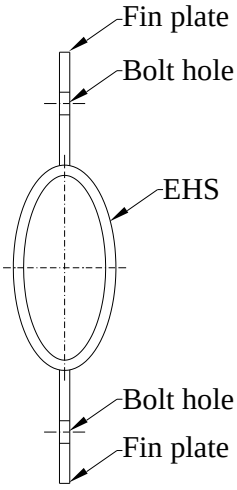

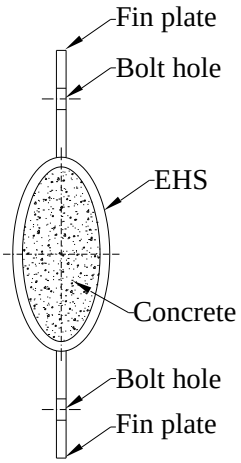

(b) Type-B: Major axis connection without stiffener

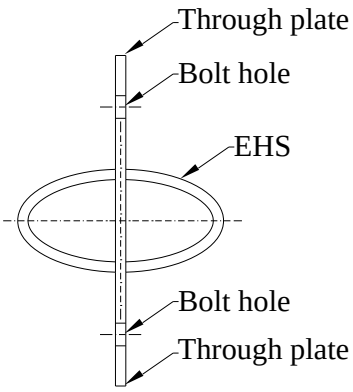

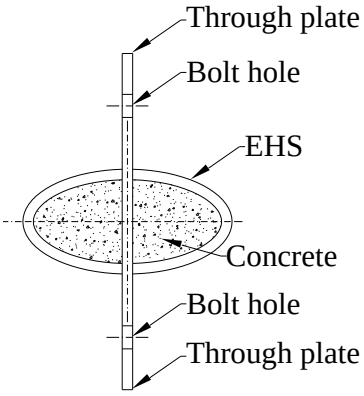

(c) Type-C: Minor axis through plate connection

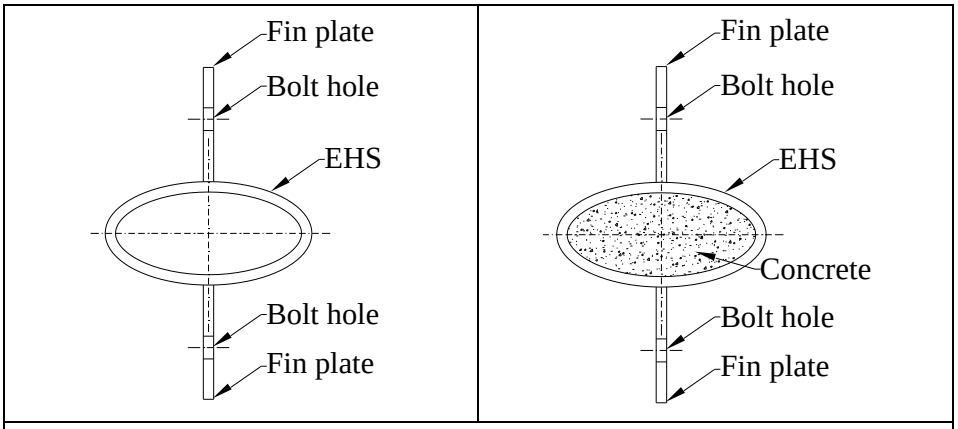

(d) Type-D: Minor axis connection without stiffener

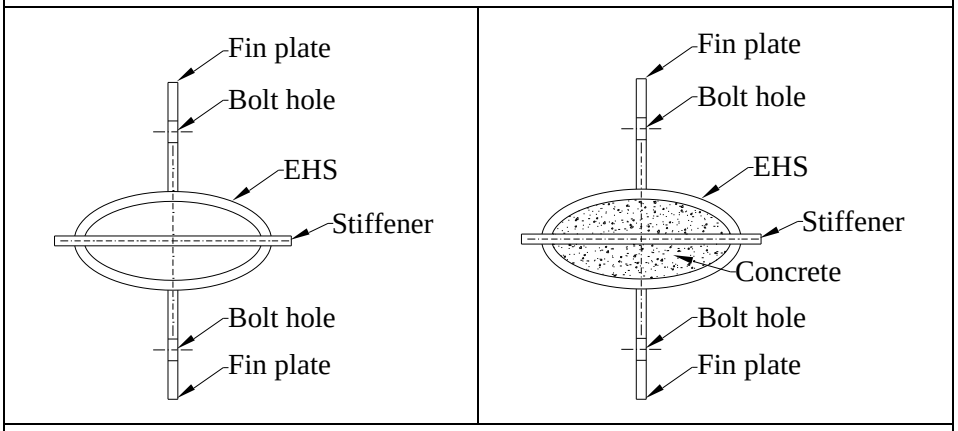

(e) Type-E: Minor axis connection with stiffener

Fig. 1. Joint assemblies (Cross-sectional view)

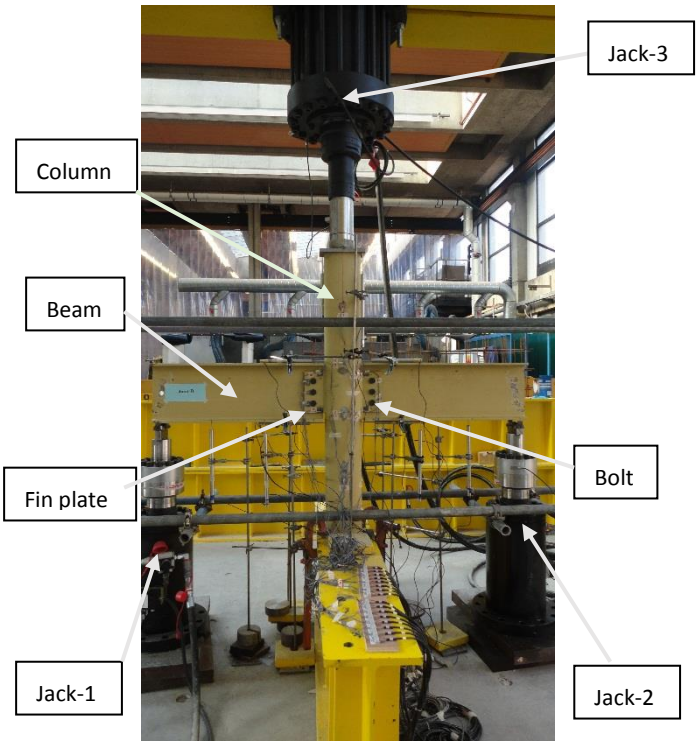

Fig. 2. Typical test setup

Fig. 3. Roller bearing

(a)	(b)	(c)

Fig. 4. Boundary conditions: (a) Top end: connecting actuator; (b) Top end: connecting EHS column; (c) Bottom end (using clamps).

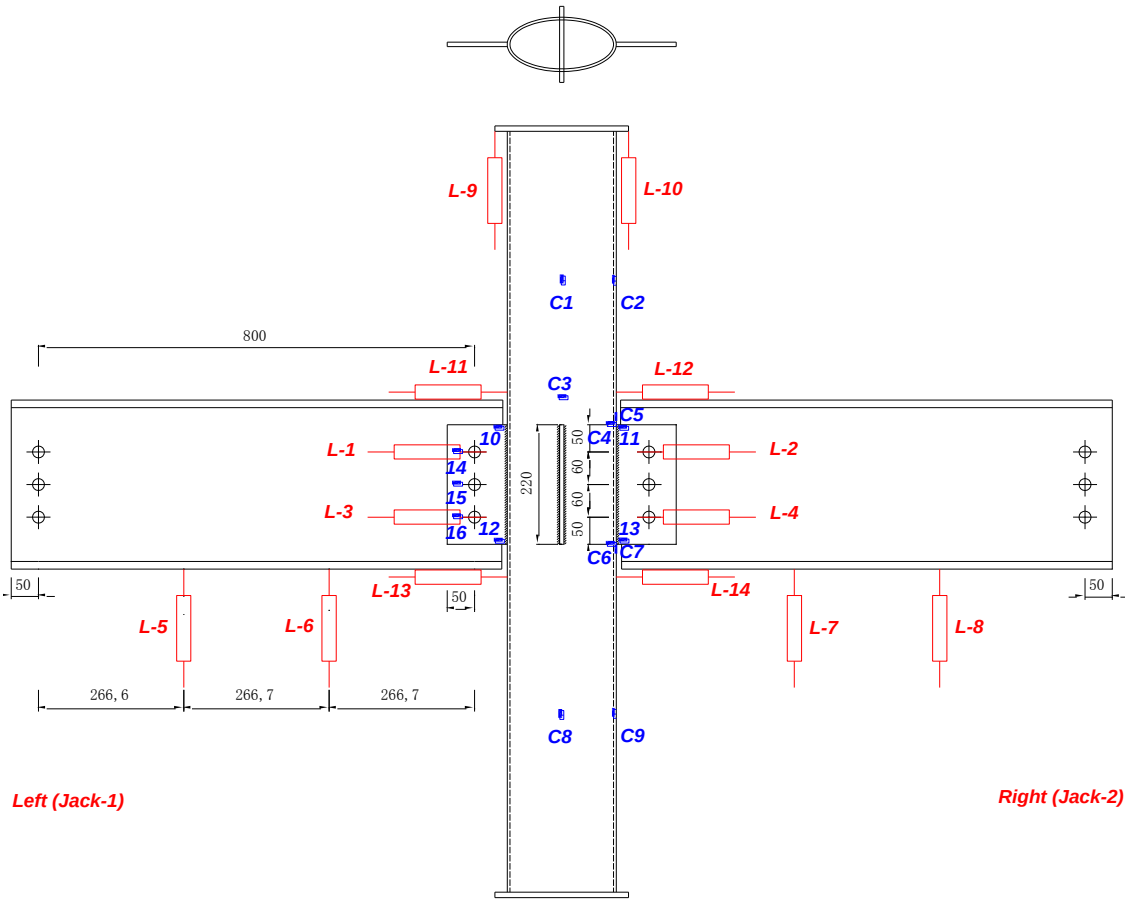

Fig. 5. Positions of Strain Gauges & LVDTs (Type-A; mm)

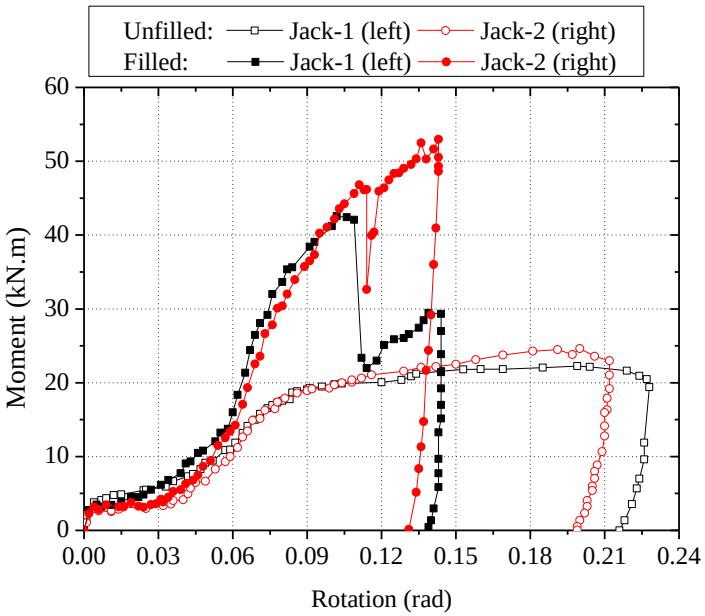

(a) Type-A connection

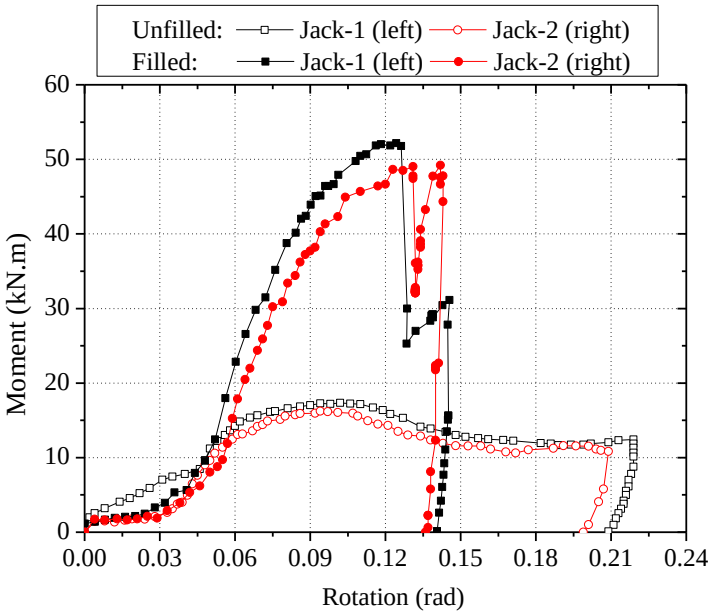

(b) Type-B connection

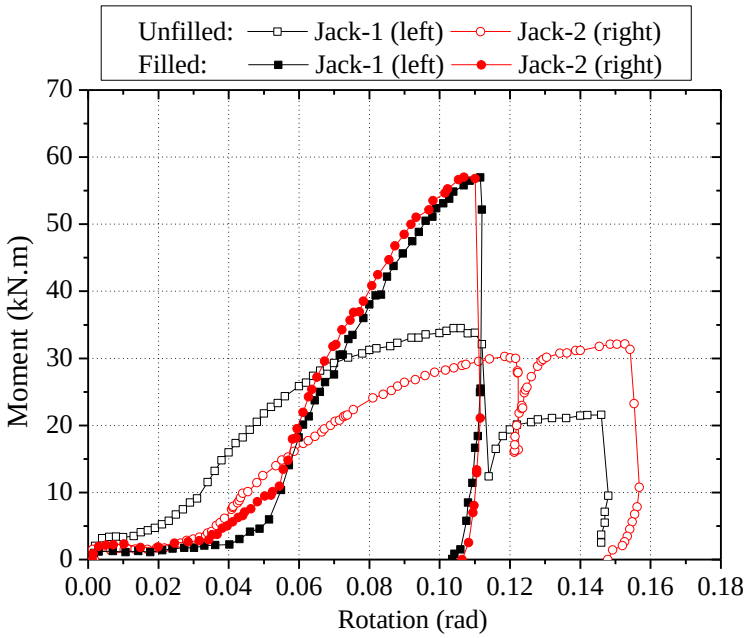

(c) Type-C connection

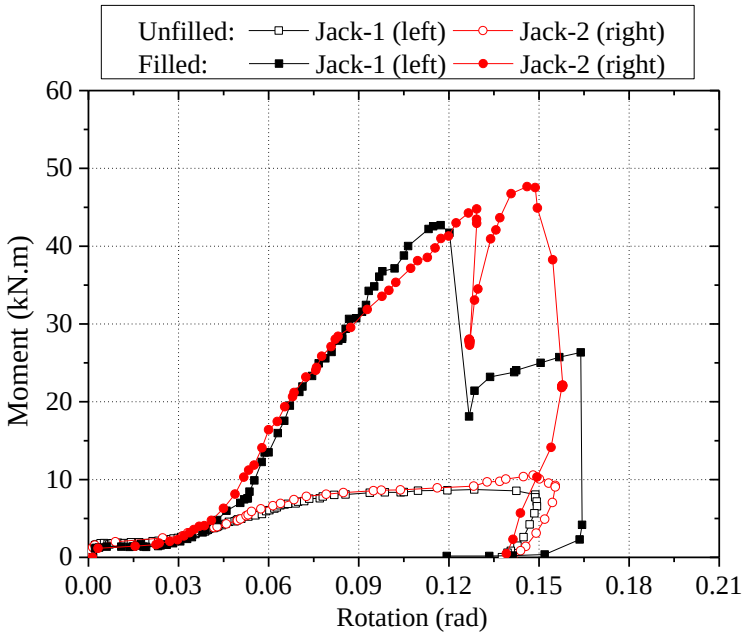

(d) Type-D connection

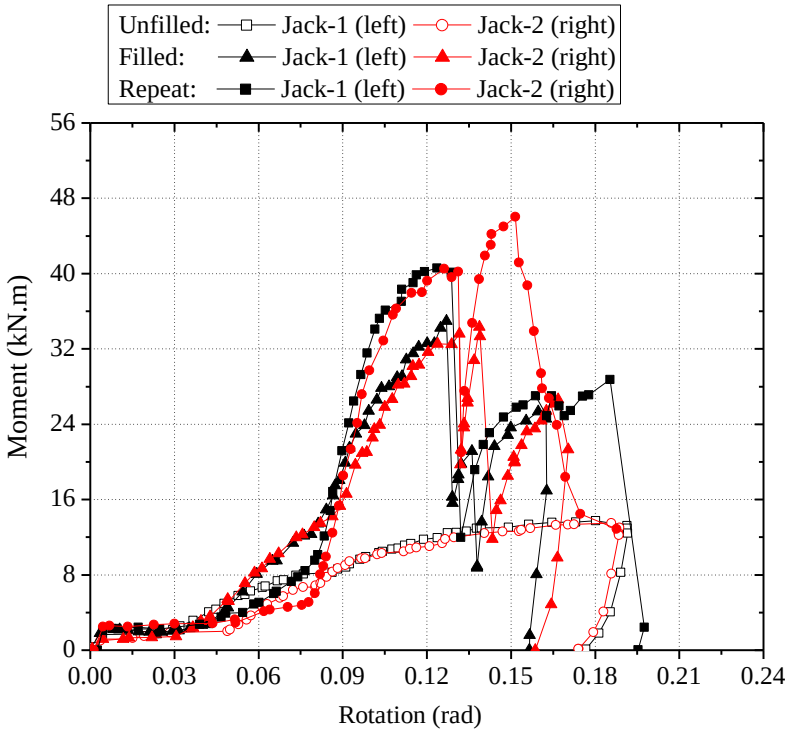

(e) Type-E connection

Fig. 6. Moment versus rotation relationships

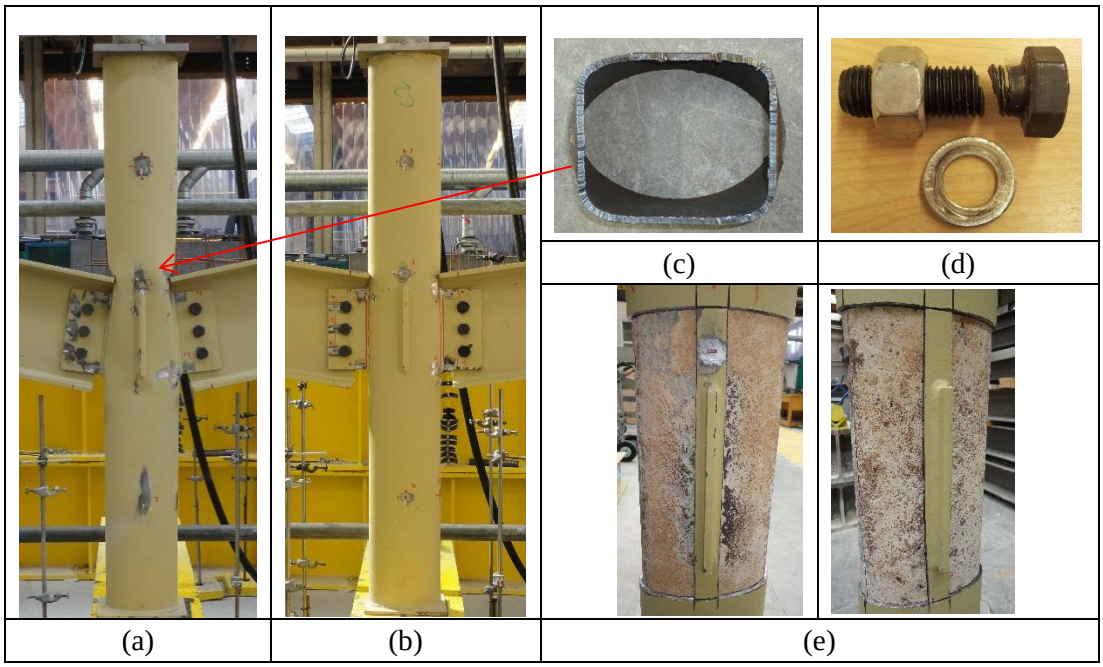

Fig. 7. Failure of Type-A connections: (a) Joint-A; (b) Joint-AC; (c) Worst section of Joint-A; (d) Bolt failure of Joint-AC; (e) Core concrete of Joint-AC

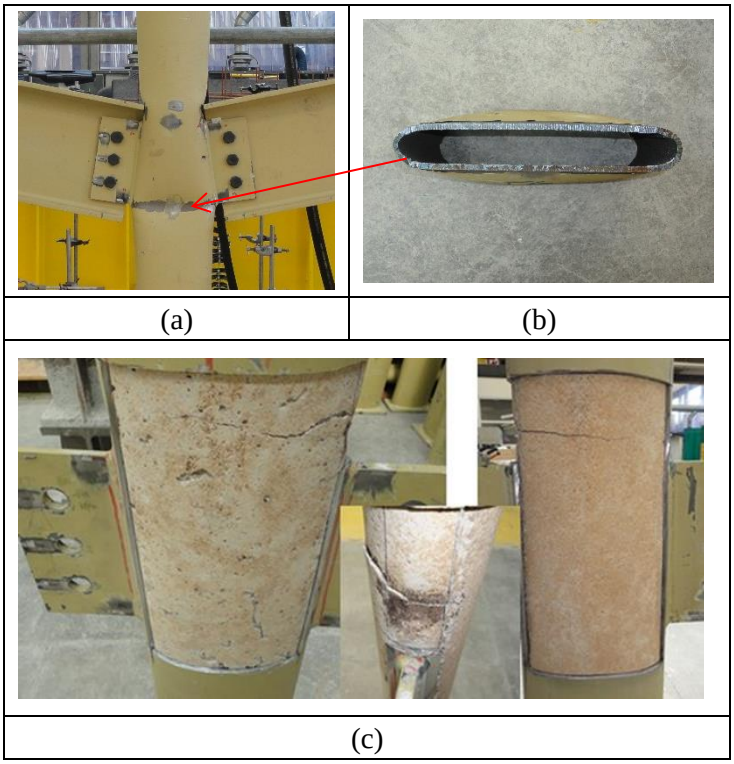

Fig. 8. Failure of Type-B connections: (a) Joint-B; (b) Bottom cross-section of Joint-B column; (c) Core concrete of Joint-BC

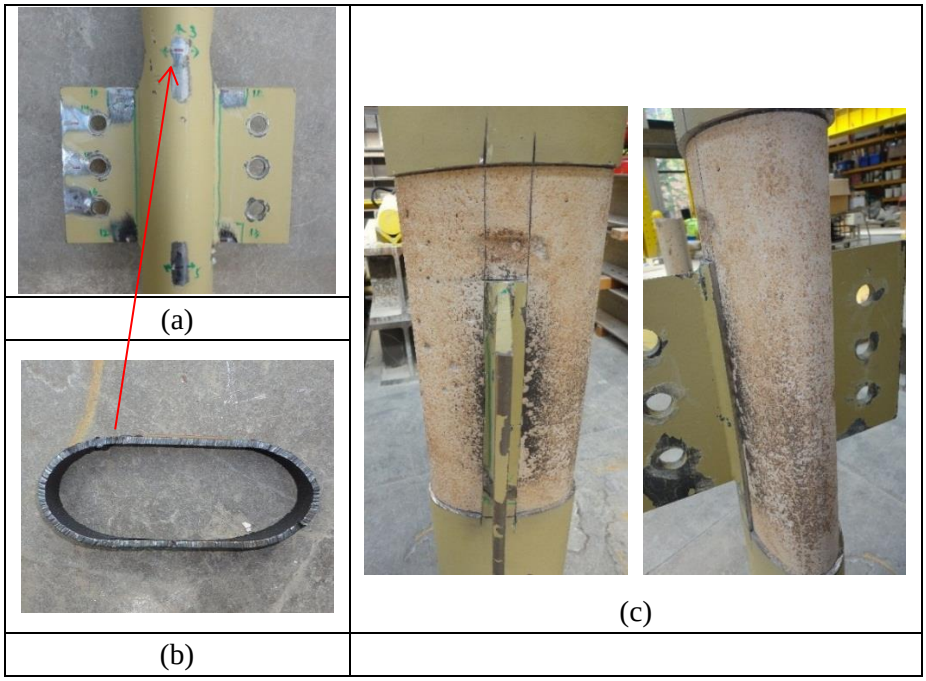

Fig. 9. Failure of Type-C connections: (a) Joint-C; (b) Top cross-section of Joint-C column; (c) Core concrete of Joint-CC

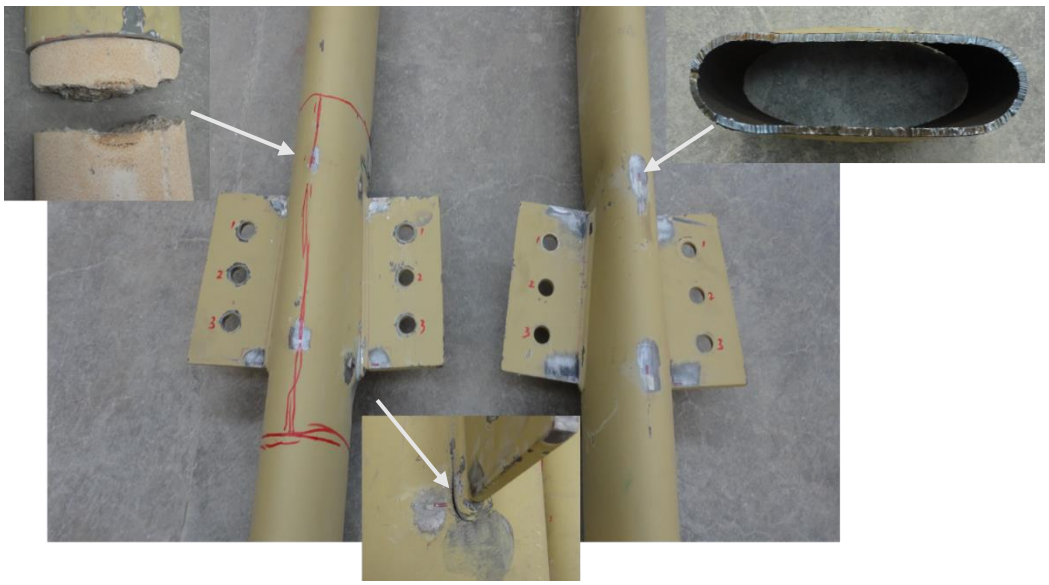

Fig. 10. Failure of Type-D connections

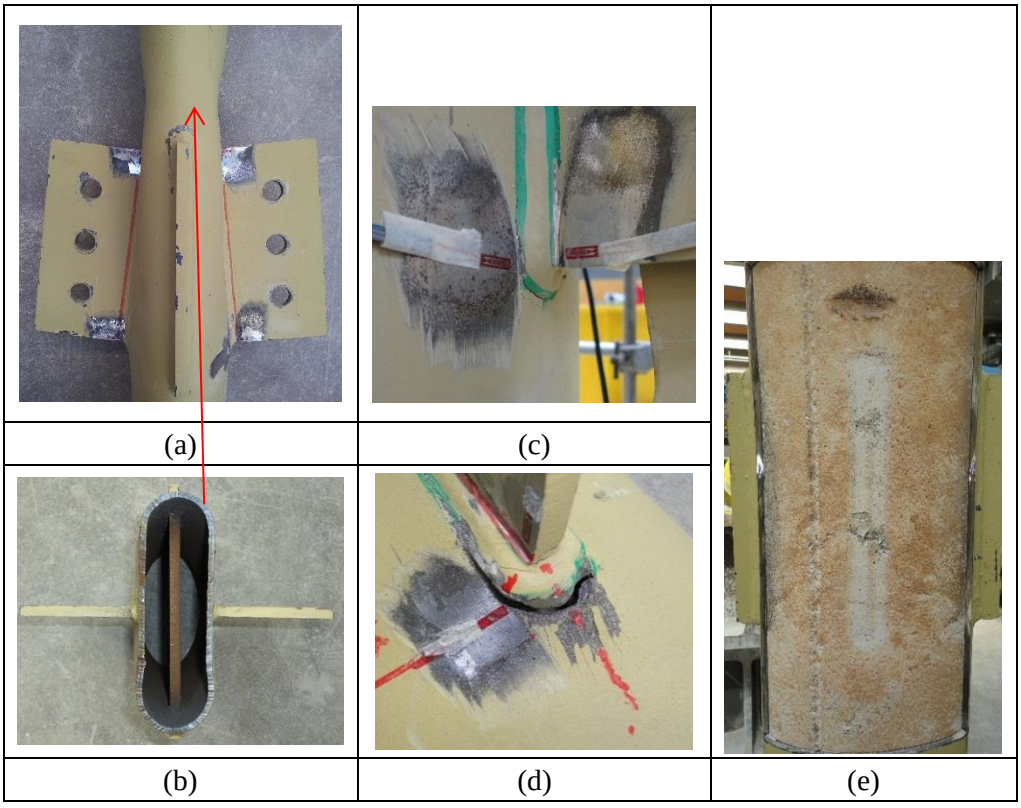

Fig. 11. Failure of Type-E connections: (a) Joint-E; (b) Top section of Joint-E column; (c) Initial cracks of Joint-EC; (d) Fracture failure of Joint-EC; (e) Core concrete of Joint-EC